Materials and Design 110 (2016) 317–323

Contents lists available at ScienceDirect

Materials and Design

journal homepage: www.elsevier.com/locate/matdes

Understanding the properties of low-cost iron-containing powder metallurgy titanium alloys

L. Bolzoni [a,*], E.M. Ruiz-Navas [b], E. Gordo [b]

[a] *WaiCAM (Waikato Centre for Advanced Materials), The University of Waikato, Private Bag 3105, 3240 Hamilton, New Zealand*
[b] *Department of Materials Science and Engineering, University Carlos III of Madrid, Avda. de la Universidad, 30, 28911 Leganes, Madrid, Spain*

HIGHLIGHTS

- Low-cost iron-containing powder metallurgy Ti-5%$_{eq.}$Fe and Ti-7%$_{eq.}$Fe alloys are designed.
- Homogeneous microstructures are obtained using the appropriate sintering parameters.
- The materials studied show mechanical behavior comparable to wrought $\alpha + \beta$ alloys.
- The novel compositions are potential candidates for cheaper structural components.

GRAPHICAL ABSTRACT

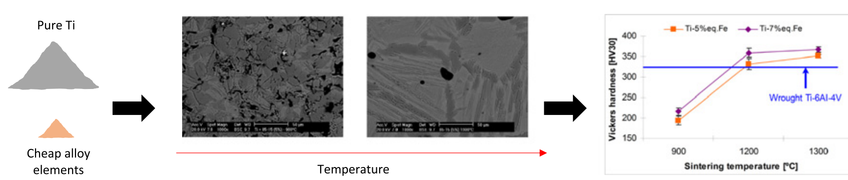

ARTICLE INFO

Article history:
Received 22 April 2016
Received in revised form 3 July 2016
Accepted 2 August 2016
Available online 3 August 2016

Keywords:
Low-cost titanium alloy
Titanium powder metallurgy
Blending elemental (BE)
Homogeneous microstructure

ABSTRACT

The high production costs of titanium in comparison to other structural metals is the main limiting factor for the wide employment of titanium. Cost reduction can be addressed considering creative fabrication methods and/or formulating new chemical compositions. In this work the fabrication of low-cost iron-containing powder metallurgy titanium alloys is studied by using a spherical 85Fe/15Ni powder whose small particle size and spherical morphology favours both the densification of the material and the diffusion of the alloying elements. The designed composition are obtained by the blending elemental approach and processed by means of the conventional powder metallurgy route. The high vacuum sintered $\alpha + \beta$ alloys show homogeneous microstructure and the formation of brittle intermetallic phases is prevented as checked by XRD and DTA analysis. Similar physical and mechanical behaviour to wrought-equivalent structural titanium alloys is obtained for these new low-cost alloys which, therefore, are potential materials for cheaper structural titanium components.

1. Introduction

Titanium has superior corrosion resistance in many aggressive chemical environments, is inert in contact with body fluids (biocompatible) and has the best specific mechanical properties among engineering metals (i.e. mechanical properties divided by density). For example, the specific strength of titanium (i.e. 288 kN m/kg) is 1.4 times and 4.5 times higher in comparison to aluminium (i.e. 204 kN m/kg) and stainless steel (i.e. 63 kN m/kg), respectively. Because of these aspects, titanium is usually employed in high demanding applications, such as in the aeronautic, naval, (petro)chemical and medicine sectors [1–3]. Nevertheless, titanium is also characterised by very high production costs which are approximately 6 times and 30 times higher, respectively, in comparison to those to obtain the same quantity of aluminium or steel [4] relegating titanium to high demanding sectors. These costs are due to the necessity to use special industrial processes to prevent the contamination of titanium from interstitials (especially oxygen and nitrogen) which are detrimental for its ductility [5,6]. Moreover, titanium is also classified as a difficult-to-machine materials as a result of its poor conductivity [7].

* Corresponding author.
E-mail address: bolzoni.leandro@gmail.com (L. Bolzoni).

http://dx.doi.org/10.1016/j.matdes.2016.08.010

The automotive industry is showing interest in the employment of titanium for the lightweighting of structural components which will eventually result in less oil consumption and lower emission of greenhouse gases [8,9]. The use of original techniques and cheap alloying elements are the two main factors which can lead to cost reduction for titanium parts [10]. Titanium and its alloys can be processed by powder metallurgy (P/M) taking advantage of the intrinsic benefits of these technologies among which the fact that they are near-net-shape methods with no need or limited need for machining operations as well as high yield (i.e. reduced generation of costly scraps). In most of the P/M methods the metal is processed well below its melting point which, in the case of titanium, is helpful to limit the reaction of titanium with the oxide- and nitride-based moulds and processing utensils. Lately, a lot of effort has been focused on developing new extraction processes, like the International Titanium Powder ITP/Armstrong [11–14], method which could be further favour the fabrication of titanium components by means of P/M techniques.

On the one hand, up to date, the titanium P/M industry has mainly focused on the production of titanium alloys whose composition is equivalent to that of commercial and well-developed wrought alloys, in particular Ti-6Al-4V. On the other hand, iron has not been completely accepted as alloying element for titanium because has higher density, and therefore tends to settle at the bottom of cast ingots and components, and the fact that is a eutectoid beta stabiliser. More in detail, above a certain percentage [15], iron forms Ti-Fe intermetallic phases which brittle the material. Nonetheless, iron is a highly desirable alloying element because stabilises the titanium beta phase (B.C.C.) and it is much cheaper than conventionally employed beta stabiliser (i.e. vanadium, tantalum and niobium). Attempts were made and some commercial wrought alloys which contemplate iron in their chemical composition can be found, such as the case of the low cost beta (LCB) developed by TIMETAL and the Ti-5Al-2.5Fe alloy. In the case of P/M processing, some few chemical compositions were studied [16–18] but the full potential of low-cost titanium alloys development has not been exploited yet. Examples are the study of Chen at al. about the effect of cooling rate on the microstructure and properties of Ti-xFe ($x = 3$, 5 and 7) produced using iron carbonyl powder [19]. Moreover, Chen and Hwang studied the formation of in situ synthesized TiC dispersoids in the sintered Ti—7Fe alloy [20].

Most of the studies available in the literature considered the effect of the addition of iron to titanium when iron was the only alloying elements but not combined with nickel. Therefore, the aim of this work was to assess the fabrication of low-cost iron-containing P/M titanium alloys produced by alloying an irregular hydride-dehydride titanium with an 85Fe/15Ni powder. The development of low-cost titanium alloys would be beneficial to widespread to use of titanium in industrial applications and potentially help to stabilise the price of titanium which is currently still primarily dependent on the fluctuation of the demand from the aeronautical sector. The iron-containing master alloy was chosen because of: (1) it is a readily availably inexpensive commercial powder, (2) the elements constituting the powder are both β-stabilisers permitting to target the production of $\alpha \pm \beta$ titanium alloys and, (3) the powder particle features of the selected master alloy favour both the densification of the material and the diffusion of the alloying elements. The starting powders were mixed, cold uniaxially pressed and sintered under high vacuum. Physical and mechanical properties of the novel low-cost iron-containing P/M titanium alloys were studied as a function of the sintering temperature. Moreover, the effect of the presence of iron and nickel as alloying elements on the phases present was assessed by differential thermal analysis (DTA) and X-ray diffraction (XRD) analysis.

2. Experimental procedure

An irregular elemental titanium powder bought from GfE GmbH (which was obtained by means of the (HDH) hydride-dehydride process) and a commercial 85Fe/15Ni powder fabricated by electrolysis (H.C. Starck) were the raw materials of the study. Important characteristics of these raw materials as well as of the mixed powders (starting materials for the study) are reported in Table 1. Specifically, two low-cost iron-containing P/M titanium alloys were designed (Ti-5$\%_{eq.}$Fe and Ti-7$\%_{eq.}$Fe).

A previous study about the addition of iron to titanium indicated that the best mechanical performances are obtained for an iron content in between 5 wt.% and 7 wt.% [18]. Most of the elements of the period table are β stabilisers, such as molybdenum, iron, manganese, chromium, nickel and vanadium. The global β stabilising effect is defined by the formula proposed by Molchanova [21], which takes into account the pondered strength of the different alloying elements:

$$[Mo]_{eq.} = [Mo] + 0.67[V] + 1.25[Cr] + 1.25[Ni] + 2.5[Fe] \quad (1)$$

From Eq. (1), alloys with 5 wt.% and 7 wt.% of iron have $[Mo]_{eq.}$ parameter of 12.5 and 17.5, respectively. These values were used to calculate to total amount of 85Fe/15Ni powder to be mixed with elemental titanium to design the two low-cost iron-containing P/M titanium alloys with an equivalent $[Mo]_{eq.}$ parameter to those of Ti-5Fe and Ti-7Fe, respectively. Specifically, they were labelled as Ti-5$\%_{eq.}$Fe and Ti-7$\%_{eq.}$Fe and their relative amount of iron and nickel (β stabilisers) are reported in Table 1. The Ti-5$\%_{eq.}$Fe and Ti-7$\%_{eq.}$Fe alloys were produced by the blending elemental approach using a Turbula mixer (processing time: 30 min). The density values of these low-cost alloys were computed by considering the rule of mixture. The density of the 85Fe/15Ni powder is much greater than that of titanium, that is why the low-cost iron-containing P/M titanium alloys have slightly higher density with respect to elemental titanium, but any possible sedimentation of heavier particle was completely prevented by compacting the Ti-5$\%_{eq.}$Fe and Ti-7$\%_{eq.}$Fe alloys samples right after mixing. From Table 1, the elemental titanium powder has irregular morphology whilst the 85Fe/15Ni powder spherical. The irregular titanium powder, which represents the great majority of the alloy, is thought to provide the backbone of the green samples (compressibility) whereas the finer 85Fe/15Ni powder particles should sit in between the spaces left from the accommodation of the asperities of the irregular titanium particles. Another important difference between the two raw materials is their particles size. The much smaller particle size of the 85Fe/15Ni powder was chosen to promote and enhance the diffusion of the alloying elements into the titanium matrix and speed up the complete homogenisation of the microstructure. Due to the chemical composition of the raw materials, the Ti-5$\%_{eq.}$Fe and Ti-7$\%_{eq.}$Fe alloys have oxygen contents of 0.29 wt.% and 0.27 wt.%, respectively. The contents of nitrogen and carbon are lower than 0.050 wt.% and 0.080 wt.%, respectively, where these values are the limits specified by ASTM standards for many titanium alloys, such as Ti-6Al-4V [22].

Table 1
Characteristics of the raw materials and mixed powders (starting materials for the study).

Characteristic		Material			
		Elemental Ti	85Fe/15Ni powder	Ti-5$\%_{eq.}$Fe	Ti-7$\%_{eq.}$Fe
Density ($\rho_{theoretical}$) [g/cm^3]		4.51	7.96	4.70	4.77
Morphology		Irregular	Spherical	–	–
Particle size distribution [μm]	D_{MAX}	<90	<10	<90	<90
	D_{10}	21.45	2.16	19.63	18.10
	D_{50}	45.80	4.36	47.89	45.69
	D_{90}	85.01	9.13	88.52	86.45
Chemical composition [wt.%]	Ti	99.6	–	Balance	Balance
	Fe	0.027	85.00	4.60	6.43
	O	0.27	–	0.29	0.27
	N	0.0080	–	0.026	0.022
	C	0.0070	–	–	–
	Ni	–	15.00	0.81	1.14

The Ti-5%$_{eq.}$Fe and Ti-7%$_{eq.}$Fe alloys starting powders were cold uniaxially pressed by means of a floating die and a uniaxial press. No lubricant was added to the powder, to limit contamination, but the walls of the die were coated with zinc stearate. The compressibility and green strength of the materials were assessed with rectangular-shaped specimens (ASTM: B528) compacted between 300 MPa and 700 MPa. Pressed green samples at 700 MPa were then chosen for further studies, such as DTA analysis (1400 °C, 10 °C/min, 40 ml/min Ar flow) and sinterability of the Ti-5%$_{eq.}$Fe and Ti-7%$_{eq.}$Fe alloys. Sintering was done in between 900 °C and 1300 °C (typical temperatures for titanium alloys sintering [23–25]) during 1 h under high vacuum (10^{-5} mbar) using 5 °C/min as heating and cooling rates. In particular, the low sintering temperature of 900 °C was selected to assess whether homogenisation of the alloying elements could be achieved and 1200 °C and 1300 °C were considered as they are common sintering temperatures for titanium $\alpha \pm \beta$ alloys. Green samples were laid on zirconia pearls placed inside an alumina tray and processed by batches.

The typical metallographic route plus etching with Kroll reagent was employed for the preparation of the specimens for microstructural analysis. Diffusion and chemical homogeneity were checked by means of SEM-EDS analysis. XRD patterns were obtained by means of a Philips X'Pert difractometer ($2\theta = 30$–$80°$, step $= 0.02°$, time per step $=$ 1.2 s). Shrinkage, densification parameter (Ψ) and relative density ($\rho_{relative}$) were the physical properties chosen to characterise the densification of the low-cost iron-containing alloys. The shrinkage was calculated as the difference between the green and the sintered samples and for that their dimensions were measured with a 2-digit calliper (length and width) and 3-digit micrometer (thickness). Green density ($\rho_{green} =$ volume/mass), relative density ($\rho_{relative} = \rho_{sintered}/\rho_{theoretical}$, where $\rho_{sintered}$ is the density of the sintered samples as measured per water displacement method and $\rho_{theoretical}$ is the theoretical density of the alloys, shown in Table 1) and $\rho_{theoretical}$ were used to compute the Ψ parameter. The amount of interstitials (i.e. oxygen and nitrogen) was measured as per ASTM: E1409 (LECO TC500). HV30 hardness measurements were carried out by means of a universal hardness tester (Wilson/Wolpert DIGITESTOR). Transverse rupture strength (TRS) values were obtained by testing the samples using a three-point bending setup (Micro-Test machine). The characterisation of the materials was performed on, at least, a minimum of three specimens in each specific test.

3. Results and discussion

Fig. 1 shows the variation of the green density (compressibility) and of the green strength of the Ti-5%$_{eq.}$Fe and Ti-7%$_{eq.}$Fe alloys powders with the applied pressure.

From Fig. 1, it can be seen that both the green density and the green strength of the Ti-5%$_{eq.}$Fe and Ti-7%$_{eq.}$Fe alloys powders increase linearly

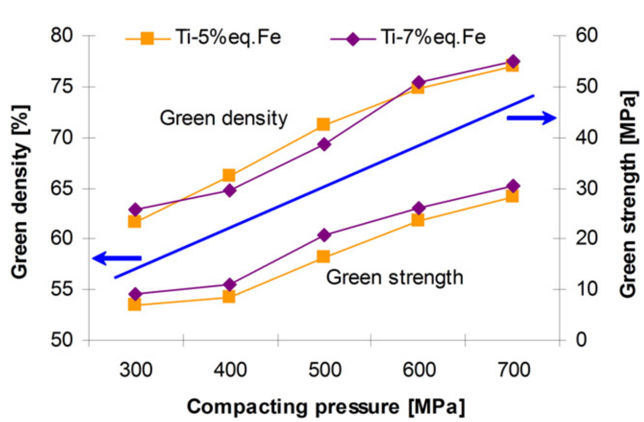

Fig. 1. Compressibility (i.e. green density) and green strength versus compacting pressure of the Ti-5%$_{eq.}$Fe and Ti-7%$_{eq.}$Fe alloys powders.

with the increment of the applied pressure. Precisely, the green density increases approximately from 60% at 300 MPa to 77% at 700 MPa where this are common values for the pressing of irregular HDH titanium powders [26]. Consequently, the volumetric amount of spherical 85Fe/15Ni powder does not seem to affect significantly the compressibility of the low-cost iron-containing P/M titanium alloys with respect to that of commercial HDH powders. This is further verified by the fact that, although there are little variations, the Ti-5%$_{eq.}$Fe and Ti-7%$_{eq.}$Fe alloys powders are characterised by similar green density values. Moreover, the presence of the spherical powder does not affect the strength of the materials which could be easily handled without breakage. Nevertheless, it can also be noticed that the green strength is higher for higher addition of 85Fe/15Ni powder (Ti-7%$_{eq.}$Fe vs. Ti-5%$_{eq.}$Fe) which could be due to the better fitting of the spherical particles into the pores left from the accommodation of the irregular titanium powder particles prior to the compaction stage.

The SEM micrographs of the sintered Ti-5%$_{eq.}$Fe and Ti-7%$_{eq.}$Fe alloys are shown in Fig. 2 and it is worth mentioning that the samples processed at 900 °C were used to assess the diffusion of the 85Fe/15Ni powder into titanium.

From Fig. 2 a) and b), it can be seen that the chemical composition of the Ti-5%$_{eq.}$Fe and Ti-7%$_{eq.}$Fe alloys is rather homogeneous although of the low sintering temperature. Only very few small undissolved particles of the 85Fe/15Ni powder could be found in the microstructure (bright spots in the micrographs, 3–5 μm). These undissolved particles are most probably the ones with the biggest size of the initially added 85Fe/15Ni powder which, due to the relatively short sintering time, did not have the change to dissolve completely. Moreover, it can be noticed that during their diffusion, the 85Fe/15Ni particles leave behind Kirkendall porosity because iron diffuses two times faster into titanium than the opposite case (Ti → Fe) [27,28]. The low-cost iron-containing Ti-5%$_{eq.}$Fe and Ti-7%$_{eq.}$Fe alloys were designed to be $\alpha + \beta$ alloys. Due to the quite efficient diffusion of iron and nickel, the microstructure of the samples sintered at 900 °C is already primarily composed of grains of the α phase (dark areas in the micrographs) and lamellae of the α and β phase (light greys areas in the micrographs) confirming that the β stabilisers (i.e. iron and nickel) are already diffused. The residual porosity of the specimens sintered at 900 °C, which is quite predominant in the microstructure, is still highly irregularly shaped and interconnected. This indicates that during the first stage of sintering the great majority of the thermal energy is spent in diffusion of the alloying elements rather than in the densification of the material. The sintering of the low-cost iron-containing Ti-5%$_{eq.}$Fe and Ti-7%$_{eq.}$Fe alloys at higher processing temperatures (1200 °C, Fig. 2 c and d, and 1300 °C, Fig. 2 e and f) leads to completely chemically homogeneous materials composed of α grains and $\alpha + \beta$ lamellae both of which become coarser with the increment of the temperature. At these processing temperatures the sintered Ti-5%$_{eq.}$Fe and Ti-7%$_{eq.}$Fe alloys show primarily spherical and isolated residual pores located at the intersection between neighbouring grains. From the comparison of the respective micrographs, the differences in terms of microstructural features which can emphasized between the Ti-5%$_{eq.}$Fe and Ti-7%$_{eq.}$Fe alloys are that the total porosity of the Ti-7%$_{eq.}$Fe alloy is lower than that of the Ti-5%$_{eq.}$Fe alloy and the lamellar spacing seems smaller. Chen at al. indicated that the lamellar spacing decreases as the amount of iron added to titanium increases [19]. It is worth mentioning that the chemical composition of the sintered materials with homogeneous microstructures was checked by means of EDS analysis (whose results are shown in Table 2) and no TiFe-based intermetallic phases were found during microstructural analysis.

From the EDS data shown in Table 2, the amount of each element of the total composition is consistent with the designed chemical composition even though there are some variations intrinsic of the semi-quantitative nature of the EDS analysis. The α phase is entirely composed of titanium, because iron and nickel have practically no solubility in α titanium [15], and the alloying elements are in the β phase which is why

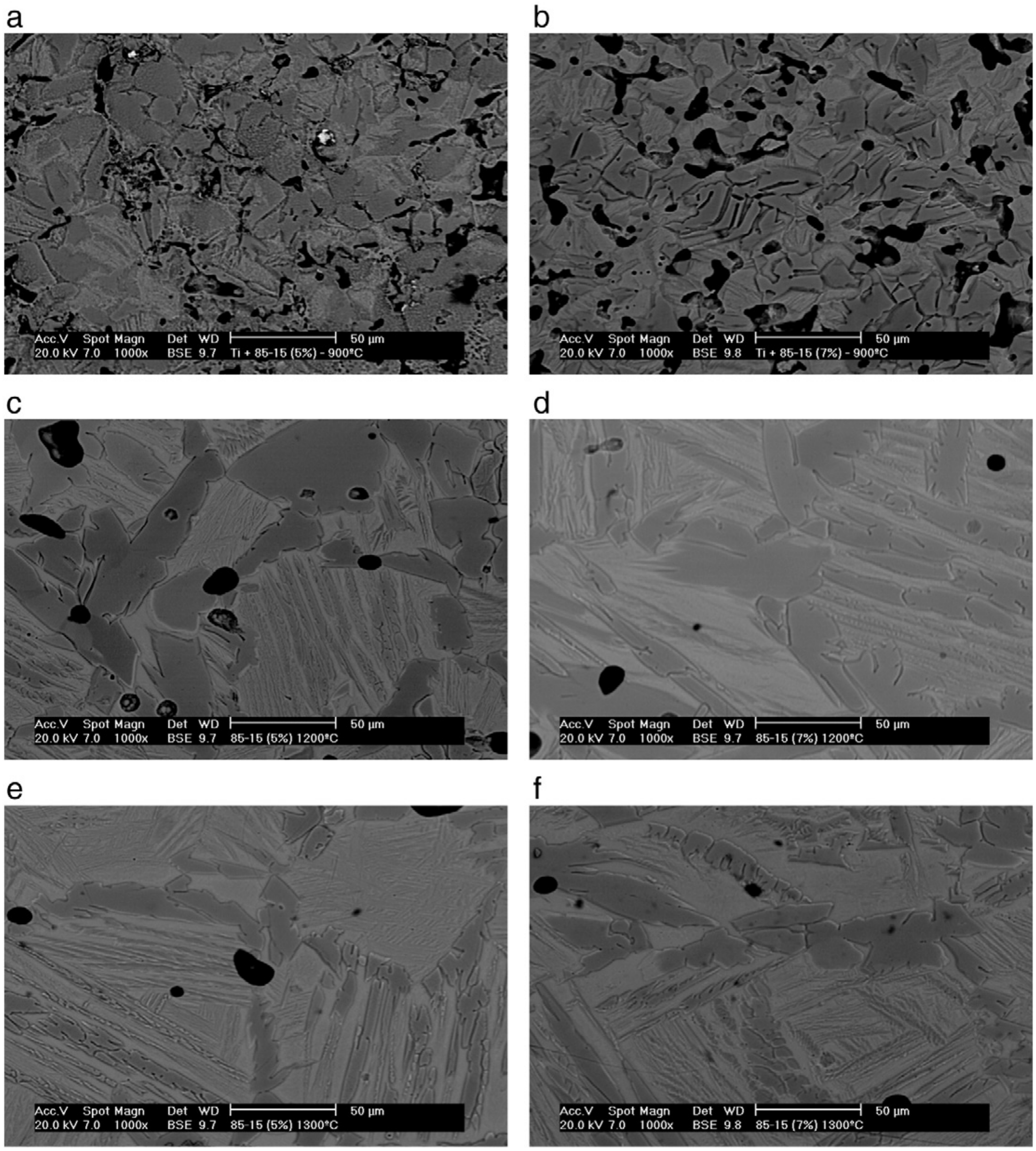

Fig. 2. SEM micrographs of the Ti-5$\%_{eq.}$Fe and Ti-7$\%_{eq.}$Fe alloys, respectively, sintered at: a) and b) 900 °C, c) and d) 1200 °C and e) and f) 1300 °C.

their amount is slightly higher with respect to the values of the total composition. In general, the atomic composition of the α and β phases of the Ti-5%eq.Fe and Ti-7%eq.Fe alloys are, respectively: (α) 100Ti and (β) 94.03Ti-4.83Fe-1.14Ni and (α) 100Ti and (β) 92.42Ti-6.11Fe-1.47Ni.

Table 2
Results of the EDS analysis performed on the Ti-5%eq.Fe and Ti-7%eq.Fe alloys samples.

Chemical composition		Ti-5%eq.Fe		Ti-7%eq.Fe	
		1200 °C	1300 °C	1200 °C	1300 °C
Total [wt.%]	Ti	Balance	Balance	Balance	Balance
	Fe	4.52	4.64	6.51	6.05
	Ni	1.2	1.02	1.47	1.6
α-phase [wt.%]	Ti	100	100	100	100
	Fe	–	–	–	–
	Ni	–	–	–	–
β-phase [wt.%]	Ti	Balance	Balance	Balance	Balance
	Fe	5.83	5.31	6.97	7.08
	Ni	1.47	1.29	1.9	1.64

The absence of TiFe-based intermetallic phases and their hindered formation was further proved by DTA analysis and the results are shown in Fig. 3.

From the DTA curves reported in Fig. 3 it can be seen that the only thermal event detected is an endothermic peak around 870 °C which corresponds to the allotropic transformation from the α to β phase of pure titanium. The transformation temperature is not affected by the presence of the alloying elements because they are not dissolved inside the titanium lattice in the Ti-5$\%_{eq.}$Fe and Ti-7$\%_{eq.}$Fe alloys powders yet during heating. Most importantly, the formation of TiFe-based intermetallic phases, as they should form on the base of the binary system (TiFe and $TiFe_2$) [15], in low-cost iron-containing Ti-5$\%_{eq.}$Fe and Ti-7$\%_{eq.}$Fe alloys does not take place. This is most probably due to the slower kinetics of the process when taking place in the solid state rather than in the liquid state and the fast diffusion of the alloying elements, although this is not the case when coarse Fe particles are used to produce low cost titanium alloys [18]. Similar behaviour was obtained when HDH titanium was alloyed with stainless steel and processed using a comparable powder metallurgy method [29].

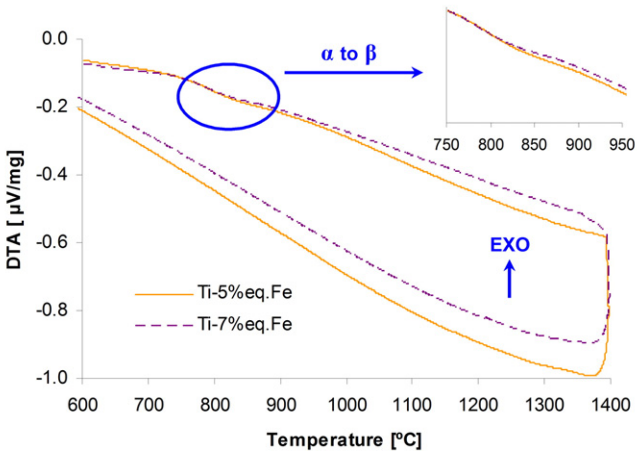

Fig. 3. DTA curves for the Ti-5%$_{eq}$Fe and Ti-7%$_{eq}$Fe alloys.

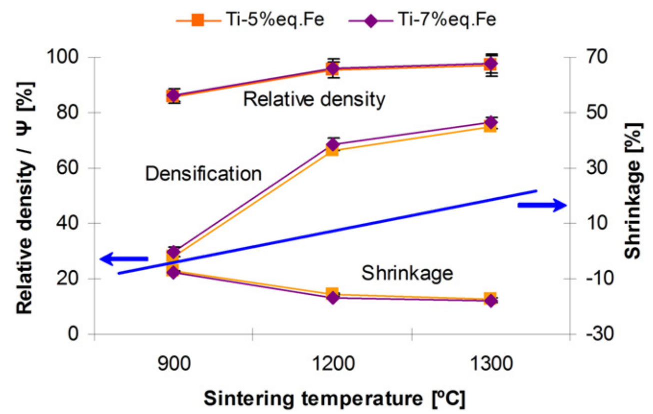

Fig. 5. Variation of shrinkage, densification parameter Ψ and relative density of the Ti-5%eq.Fe and Ti-7%eq.Fe alloys with the sintering temperature.

A further assessment of the phases that comprise the low-cost iron-containing Ti-5%$_{eq}$Fe and Ti-7%$_{eq}$Fe alloys was done by means of XRD analysis and the patterns are presented in Fig. 4.

From the XRD patterns of the sintered Ti-5%$_{eq}$Fe and Ti-7%$_{eq}$Fe alloys it can be seen that the phases that compose the low-cost iron-containing P/M titanium alloys are α and β titanium. No important differences are found between the Ti-5%$_{eq}$Fe and the Ti-7%$_{eq}$Fe alloys independently of the sintering temperature employed if not that the intensity of the main β-Ti peak (i.e. 100 plane) is higher for theTi-7%$_{eq}$Fe alloy. This is in agreement with the fact that the higher the amount of β stabilisers contemplated in the chemical composition of the alloy the higher the relative amount of β phase that characterise them. By means of the XRD patterns it is further verified that TiFe-based intermetallic phases are not present, which is especially relevant for an addition of 7 wt.% of iron. A similar trend where no TiFe-based intermetallic phases were formed and the intensity of the β peaks increased with the amount of iron added due to the stabilising effect of iron on the titanium β-phase was found in binary Ti-xFe alloy [19].

Fig. 5 shows the variation of the shrinkage, densification parameter (Ψ) and relative density of the Ti-5%$_{eq}$Fe and the Ti-7%$_{eq}$Fe alloys with the sintering temperature.

From Fig. 5, the sintering of the Ti-5%$_{eq}$Fe and the Ti-7%$_{eq}$Fe alloys leads to the shrinkage of the materials where the contraction increases along with the sintering temperature ranging between 7% at 900 °C and 18% at 1300 °C. The relatively low contraction of the materials at 900 °C is imputable to the fact that most of the thermal energy is invested in homogenisation of the alloying elements rather than in self-diffusion of the coarser titanium powder particles. This could be expected on the base of the microstructural analysis (Fig. 2). Consequently, the highest increment in shrinkage is seen when increasing the processing temperature from 900 °C to 1200 °C (i.e. 16%) and a further increment of the temperature to 1300 °C does not increase significantly the shrinkage (i.e. 18%). From the comparison of the two low-cost iron-containing P/M titanium alloys, Ti-7%$_{eq}$Fe alloy undergoes slightly higher contraction (0.7% on average) with respect to the Ti-5%$_{eq}$Fe alloy which is due to the greater relative amount of finer powder particles (i.e. 85Fe/15Ni powder) present in the alloy. The densification of the materials increases with the processing temperature and, once again, the most important change happens from 900 °C to 1200 °C. As previously explained, this behaviour is related to the competition between the interdiffusion of the alloying elements towards titanium and the self-diffusion of titanium which also explains the somewhat higher densification of the Ti-7%$_{eq}$Fe alloy (1.9% on average) compared to the Ti-5%$_{eq}$Fe alloy. From Fig. 5, the relative density of the Ti-5%$_{eq}$Fe and the Ti-7%$_{eq}$Fe alloys increases with the sintering temperature as this property is related to the shrinkage and densification of the materials. The samples sintered at 900 °C are characterised by quite low relative density (approximately 86%) due low processing temperature although the chemical composition is already rather homogeneous (Fig. 2). Due to the higher densification that the material experiences, the Ti-7%$_{eq}$Fe alloy generally shows a little bit higher relative density (i.e. 0.5%) with respect to the Ti-5%$_{eq}$Fe alloy. The final relative density values of both the low-cost iron-containing P/M titanium alloys are comparable to those of wrought-equivalent titanium alloys processed by pressing and sintering [17,26,30–34]. It is worth mentioning, in particular, relative density values of 97% were obtained in iron-containing powder metallurgy titanium alloys by using finer powders (25 µm spherical titanium mixed with 3 µm iron carbonyl powder) combined with lower sintering temperature (i.e. 1150 °C) but longer dwell time (i.e. 2 h) [19,20].

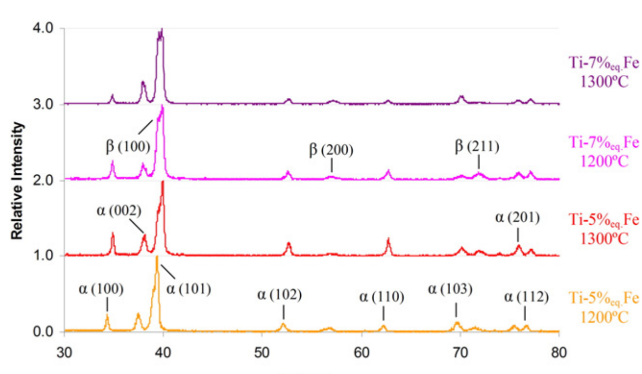

Fig. 4. XRD patterns of the sintered Ti-5%$_{eq}$Fe and Ti-7%$_{eq}$Fe alloys.

Oxygen and nitrogen contents of the sintered Ti-5%$_{eq}$Fe and the Ti-7%$_{eq}$Fe alloys are shown in Table 3 where it can be seen that the total amount of these two interstitials remains almost constant at approximately 0.53 wt.% and 0.09 wt.%, respectively, regardless of the processing temperature employed to sinter the low-cost iron-containing P/M titanium alloys. Moreover, it can be noticed that there is quite an important interstitials pick-up in comparison to the values of the starting

Table 3
Oxygen and nitrogen contents of the sintered Ti-5%eq.Fe and Ti-7%eq.Fe alloys.

Alloy		Chemical composition	
		O [wt.%]	N [wt.%]
Ti-5%$_{eq}$Fe	900 °C	0.54 ± 0.02	0.094 ± 0.014
	1200 °C	0.52 ± 0.01	0.108 ± 0.033
	1300 °C	0.50 ± 0.04	0.104 ± 0.003
Ti-7%$_{eq}$Fe	900 °C	0.54 ± 0.01	0.075 ± 0.013
	1200 °C	0.53 ± 0.03	0.087 ± 0.022
	1300 °C	0.56 ± 0.07	0.092 ± 0.005

powders (Table 1). This is due to the nitrogen and, especially, oxygen atoms adsorbed into the surface of the powder particles, whose amount is higher for finer particles because they have higher surface energy, and the air trapped inside the porosity of the green samples which diffuses inward during the sintering step.

The variation of the Vickers hardness with the sintering temperature (Fig. 6) shows that the low-cost iron-containing P/M titanium alloys becomes harder with the increment of the processing temperature. This increment is due to the combined effect of higher relative density, or in turns lower volumetric percentage of residual porosity distributed in the microstructure, and the total amount of alloying elements and interstitials because oxygen and nitrogen harden titanium [5,6].

From the comparison of the two low-cost iron-containing P/M titanium alloys, the Ti-7%$_{eq}$Fe alloy is always characterised by higher hardness (roughly 20 HV30) than the Ti-5%$_{eq}$Fe alloy clearly highlighting the effect of the total amount of alloying elements (i.e. beta stabilisers) added. The hardness values are also affected by the slightly differences in terms of relative density (Fig. 5) and interstitials content (Table 3) which harden titanium [5,6]. As described on the base of the microstructural analysis (Fig. 2), the low-cost iron-containing P/M titanium alloys are $\alpha + \beta$ titanium alloys because both iron and nickel are β stabilisers but their total amount is not sufficiently high as to create a metastable or stable β titanium alloy as normally > 15% and 30% of β stabilisers are required, respectively [22]. Consequently, the mechanical properties of the Ti-5%$_{eq}$Fe and the Ti-7%$_{eq}$Fe alloys can be compared to those of the most famous $\alpha + \beta$ titanium alloy, the Ti-6Al-4V alloy. From Fig. 6, it can be seen that the low-cost iron-containing P/M titanium alloys have higher hardness with respect to the wrought Ti-6Al-4V alloy (i.e. 321 HV [22]), with the exception of the samples sintered at 900 °C, albeit of the presence of the residual porosity as microstructural feature. This behaviour is once again related to the chemical composition of the materials and, specifically, to the much higher amount of interstitials of the Ti-5%$_{eq}$Fe and the Ti-7%$_{eq}$Fe alloys in comparison to the wrought Ti-6Al-4V alloy (i.e. $O_{MAX} = 0.20$ wt.% and $N_{MAX} = 0.050$ wt.% [22]). Similar behaviour and hardness values as the ones reported in Fig. 6 were obtained when HDH pure titanium was mixed with a 430 stainless steel powder due to the effect of the β-stabilising elements added (i.e. Fe, Cr, Si and Mn) [29].

The results of the three-point bending tests performed on the sintered Ti-5%$_{eq}$Fe and the Ti-7%$_{eq}$Fe alloys samples are displayed in Fig. 7.

From Fig. 7 a), the low-cost iron-containing P/M titanium alloys are characterised by similar behaviour mainly deforming elastically with the increment of the applied load and with some plastic deformation prior fracture. Moreover, since the curves of the two materials overlie, the Ti-5%$_{eq}$Fe and the Ti-7%$_{eq}$Fe alloys have similar elastic modulus. From the analysis of the mechanical properties of the materials with the sintering temperature (Fig. 7 b) it can be seen that the TRS decreases

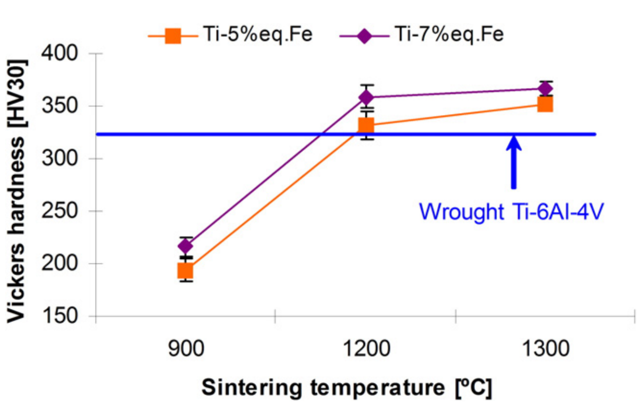

Fig. 6. Variation of the Vickers hardness of the Ti-5%eq.Fe and Ti-7%eq.Fe alloys. with the sintering temperature.

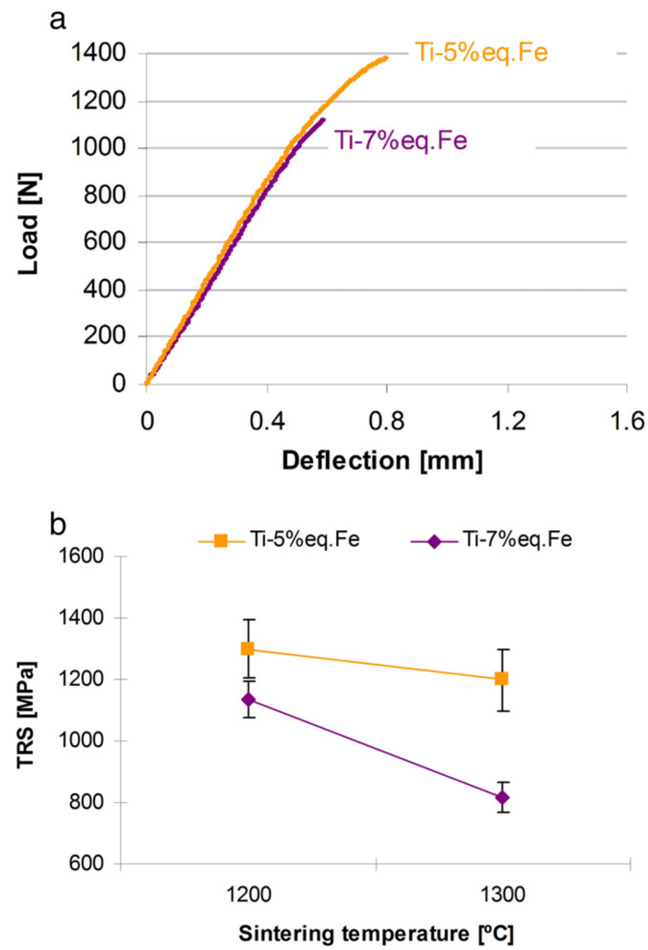

Fig. 7. Results of the three-point bending tests performed on the sintered Ti-5%$_{eq}$Fe and Ti-7%$_{eq}$Fe alloys samples: a) representative load-deflection curves (1200 °C) and b) TRS vs. sintering temperature.

with the increment of the processing temperature. Although of its higher relative density, the Ti-7%$_{eq}$Fe alloy shows lower mechanical performances with respect to the Ti-5%$_{eq}$Fe alloy independently of the sintering temperature. The decreasing behaviour of the mechanical performances is due to the contrasting effect of the residual porosity, the increment of the interstitials (in particular oxygen) and the coarsening of the microstructural features with the increment of the sintering temperature. Specifically, the pore size increases in the final stage of sintering and both the size of the prior β grains and the width and length of the $\alpha \pm \beta$ undergoes growth reducing the lamellae spacing and inducing a reduction of the strength of the alloys. The trends of the TRS and the values obtained when alloying titanium with Fe/Ni are comparable to those of low-cost titanium alloys developed by adding a commercial stainless steel powder [29]. Excepted the Ti-7%$_{eq}$Fe alloy sintered at 1300 °C, the two low-cost iron-containing P/M titanium alloys have higher TRS in comparison to the values of wrought biomedical devices made out of the Ti-6Al-4V (903–1090 MPa) and Ti-6Al-7Nb (935–995 MPa) alloys [35].

4. Conclusions

From this work about the alloying of elemental titanium with 85Fe/15Ni to produce low-cost iron-containing powder metallurgy (P/M) titanium alloys it can be concluded that the studied compositions are promising alternatives to fabricate cheap non-critical structural titanium components. The addition of fine 85Fe/15Ni powder to titanium does not compromise the handability of the green samples and simultaneously enhances the homogenisation of the alloying elements and the densification of the material. Completely homogeneous microstructure are obtained from sintering temperature of 1200 °C and the formation of brittle TiFe-based intermetallic phases is prevented by using the P/M route of pressing and sintering. Furthermore, the sintered low-cost iron-containing Ti-5%$_{eq.}$Fe and the Ti-7%$_{eq.}$Fe alloys are characterised by physical and mechanical properties, especially in terms of strength, comparable to those of other wrought-equivalent and low-cost P/M titanium alloys.

Acknowledgements

The authors want to acknowledge the starting support from New Zealand Ministry of Business, Innovation and Employment (MBIE) (UOWX1402) through the TiTeNZ (Titanium Technologies New Zealand) research contract.

References

[1] G. Lütjering, J.C. Williams, Titanium: Engineering Materials and Processes, first ed. Springer, Manchester, UK, 2003.
[2] V.A. Joshi, Titanium Alloys: An Atlas of Structures and Fracture Features: Taylor & Francis, 2006.
[3] D.M. Brunette, P. Tengvall, M. Textor, P. Thomsen, Titanium in Medicine: Materials Science, Surface Science, Engineering, Biological Responses and Medical Applications, Springer, New York, USA, 2001.
[4] K. Faller, F.S. Froes, The use of titanium in family automobiles: current trends, JOM 53 (2001) 27–28.
[5] R.I. Jaffee, I.E. Campbell, The effect of oxygen, nitrogen and hydrogen on iodide refined titanium, Transactions of the American Institute of Mining and Metallurgical Engineers, 185, 1949, pp. 646–654.
[6] R.I. Jaffee, H.R. Ogden, D.J. Maykuth, Alloys of titanium with carbon, oxygen and nitrogen, Transactions of the American Institute of Mining and Metallurgical Engineers, 188, 1950, pp. 1261–1266.
[7] I.J. Polmear, Light Alloys. From Traditional Alloys to Nanocrystals, fourth ed. Butterworth-Heinemann, UK, 2006.
[8] E.H. Kraft, Opportunities for Low Cost Titanium in Reduced Fuel Consumption, Improved Emissions, and Enhanced Durability Heavy-duty Vehicles. Subcontract 4000013062. Vancouver, WA 98664, EHKTechnologies, USA, 2002 (Available at:) http://www.ornl.gov/sci/propulsionmaterials/pdfs/Low-CostTitanium.pdf.
[9] C.A. Lavender, Low-cost Titanium Evaluation, FY 2004 Progress Report, Automotive Lightweighting Materials, Office of Freedom Car and Vehicle Technologies, 2005 (Available online at) http://www1.eere.energy.gov/vehiclesandfuels/pdfs/alm_04/3e_lavender.pdf.
[10] T.E. Norgate, G. Wellwood, The potential applications for titanium metal powder and their life cycle impacts, JOM 58 (2006) 58–63.
[11] S.J. Gerdemann, Titanium process technologies, Adv. Mater. Processes 159 (2001) 41–43.
[12] G. Crowley, How to extract low-cost titanium, Adv. Mater. Processes 161 (2003) 25–27.
[13] W.H. Peter, C.A. Blue, C.R. Scorey, W. Ernst, J.M. McKernan, J.O. Kiggans, et al., Non-melting Processing of "Low-cost" Armstrong Titanium and Titanium Alloy Powders. Proceedings of the Light Metals Technology Conference 2007(Saint-Sauveur, Québec, Canada) 2007.
[14] C.A. Lavender, K.S. Weil, Low-cost titanium powder for feedstock, FY 2007 Progress Report CPNnl, Automotive Lightweighting Materials, 2007 (available at:) http://www1.eere.energy.gov/vehiclesandfuels/pdfs/lm_07/4_automotive_metals-titanium.pdf;.
[15] F.H. Froes, Titanium: Physical Metallurgy, Processing and Applications, Ohio, USA, 2015.
[16] H. Hotta, M. Abe, T. Kuji, H. Uchida, Synthesis of Ti-Fe alloys by mechanical alloying, J. Alloys Compd. 439 (2007) 221–226.
[17] O.M. Ivasishin, Cost-effective manufacturing of titanium parts with powder metallurgy approach, Materials Forum 29 (2005) 1–8.
[18] P.G. Esteban, L. Bolzoni, E.M. Ruiz-Navas, E. Gordo, PM processing and characterisation of Ti-7Fe low cost titanium alloys, Powder Metall. 54 (2011) 242–252.
[19] B.-Y. Chen, K.-S. Hwang, K.-L. Ng, Effect of cooling process on the alpha phase formation and mechanical properties of sintered Ti-Fe alloys, Mater. Sci. Eng. A 528 (2011) 4556–4563.
[20] B.-Y. Chen, K.-S. Hwang, Sintered Ti-Fe alloys with in situ synthesized TiC dispersoids, Mater. Sci. Eng. A 541 (2012) 88–97.
[21] K. Molchanova, Phase Diagrams of Titanium Alloys. Translation of Atlas Diagram Sostoyaniya Titanovyk Splavov, Israel Program for Scientific Translations, Jerusalem, 1965 154.
[22] R. Boyer, G. Welsch, E.W. Collings, Materials properties handbook: titanium alloys, International A, second ed., 1998 (Ohio, USA).
[23] M. Holm, T. Ebel, M. Dahms, Investigations on Ti-6Al-4V with gadolinium addition fabricated by metal injection moulding, Mater. Des. 51 (2013) 943–948.
[24] Y.F. Yang, S.D. Luo, G.B. Schaffer, M. Qian, Sintering of Ti–10V–2Fe–3Al and mechanical properties, Mater. Sci. Eng. A 528 (2011) 6719–6726.
[25] R.P. Siqueira, H.R.Z. Sandim, V.A.R. Henriques, J.F.C. Lins, Microstructural Evolution during Sintering of the P/M Blended Elemental Ti-5Al-2.5Fe Alloy. Advanced Powder Technology IV, 55–60, 2005 498–499.
[26] L. Bolzoni, E.M. Ruiz-Navas, E. Gordo, Flexural properties, thermal conductivity and electrical resistivity of prealloyed and master alloy addition powder metallurgy Ti-6Al-4V, Mater. Des. 52 (2013) 888–895.
[27] H. Nakajima, K. Yusa, Y. Kondo, Diffusion of iron in a diluted [alpha]-Ti-Fe alloy, Scr. Mater. 34 (1996) 249–253.
[28] H. Nakajima, S. Ohshida, K. Nonaka, Y. Yoshida, F.E. Fujita, Diffusion of iron in [beta] Ti-Fe alloys, Scr. Mater. 34 (1996) 949–953.
[29] L. Bolzoni, E. Herraiz, E.M. Ruiz-Navas, E. Gordo, Study of the properties of low-cost powder metallurgy titanium alloys by 430 stainless steel addition, Mater. Des. 60 (2014) 628–636.
[30] V.A.R. Henriques, P.P. de Campos, C.A. Alves Cairo, J.C. Bressiani, Production of titanium alloys for advanced aerospace systems by powder metallurgy, Mater. Res. 8 (2005) 443–446.
[31] Y. Liu, L.F. Chen, H.P. Tang, C.T. Liu, B. Liu, B.Y. Huang, Design of powder metallurgy titanium alloys and composites, Mater. Sci. Eng. A 418 (2006) 25–35.
[32] S. Abkowitz, D. Rowell, Superior fatigue properties for blended elemental P/M Ti-6Al-4V, JOM 38 (1986) 36–39.
[33] L. Bolzoni, P.G. Esteban, E.M. Ruiz-Navas, E. Gordo, Mechanical behaviour of pressed and sintered titanium alloys obtained from master alloy addition powders, J. Mech. Behav. Biomed. Mater. 15 (2012) 33–45.
[34] F.H. Froes, O.M. Ivasishin, V.S. Moxson, D.G. Savvakin, K.A. Bondareva, A.M. Demidik, Cost-effective Synthesis of Ti–6Al–4V Alloy Components via the Blended Elemental P/M Approach, in: TMS, W. PA (Ed.), Symposium on TMS Symposium on High Performance Metallic Materials for Cost Sensitive Applications, 2002 (Seattle, WA).
[35] D. Henry, Materials and Coatings for Medical Devices: Cardiovascular, Ohio, USA, ASM International, 2009.